



Thymoquinone and Costunolide Induce Apoptosis of Both Proliferative and Doxorubicin-Induced-Senescent Colon and Breast Cancer Cells

Integrative Cancer Therapies
Volume 20: 1–20
© The Author(s) 2021
Article reuse guidelines:
sagepub.com/journals-permissions
DOI: 10.1177/15347354211035450
journals.sagepub.com/home/ict


Ali H El-Far, PhD¹ , Kavitha Godugu, PhD², Ahmed E. Noreldin, PhD¹, Amna A. Saddiq, PhD³, Omar A. Almaghrabi, PhD³, Soad K. Al Jaouni, PhD⁴, and Shaker A. Mousa, PhD, MBA, FACC, FACB²

Abstract

Doxorubicin (Dox) induces senescence in numerous cancer cell types, but these senescent cancer cells relapse again if they are not eliminated. On this principle, we investigated the apoptotic effect of thymoquinone (TQ), the active ingredient of *Nigella sativa* seeds and costunolide (COS), the active ingredient of *Costus speciosus*, on the senescent colon (Sen-HCT116) and senescent breast (Sen-MCF7) cancer cell lines in reference to their corresponding proliferative cells to rapidly eliminate the senescent cancer cells. The senescence markers of Sen-HCT116 and Sen-MCF7 were determined by a significant decrease in bromodeoxyuridine (BrdU) incorporation and significant increases in SA- β -gal, p53, and p21 levels. Then proliferative, Sen-HCT116, and Sen-MCF7 cells were subjected to either TQ (50 μ M) or COS (30 μ M), the Bcl2-associated X protein (Bax), B-cell lymphoma 2 (Bcl2), caspase 3 mRNA expression and its activity were established. Results revealed that TQ significantly increased the Bax/Bcl2 ratio in HCT116 + Dox5 + TQ, MCF7 + TQ, and MCF7 + Dox5 + TQ compared with their corresponding controls. COS significantly increased the Bax/Bcl2 ratio in HCT116 + Dox5 + TQ and MCF7 + Dox5 + TQ compared with their related controls. Also, TQ and COS were significantly increased caspase 3 activity and cell proliferation of Sen-HCT116 and Sen-MCF7. The data revealed a higher sensitivity of senescent cells to TQ or COS than their corresponding proliferative cells.

Keywords

thymoquinone, costunolide, senescence, apoptosis

Submitted February 3, 2021; revised June 23, 2021; accepted July 9, 2021

Introduction

The principal bioactive ingredient of *Nigella sativa* seeds is thymoquinone (TQ), which has several biological activities such as antioxidant, anticancer, and anti-toxicant.^{1–6} TQ prompted apoptosis of the human colon cancer (HCT116) cell line via a p53 dependence.⁷ Also, TQ induced apoptosis in a human breast cancer cell line (MCF7) through the upregulation of p53 in a time-dependent manner.⁸ Moreover, TQ inhibited B-cell lymphoma 2 (Bcl2), which is anti-apoptotic in both in vitro and in vivo cancer models.⁹

Costunolide (COS) is a natural sesquiterpene lactone isolated from *Costus speciosus* roots with anti-inflammatory, antioxidant, and anticancer effects.¹⁰ COS targeted many essential macromolecules, such as mitogen-activated protein kinases, protein kinase B, nuclear factor- κ B, transcription signal transducer, and activator and activator protein-1.¹¹ Also, COS at doses of 40 and 80 μ M induced

apoptosis of human lung squamous carcinoma cell line (SK-MES-1) through increases of p53 and Bax expressions and decreases of Bcl2 expression.¹² Similarly, significant upregulation of caspase 3 and caspase 9, which enhanced the apoptosis of breast cancer cell lines (MCF7 and MDA-MB-231), were recognized.¹³

¹Damanhour University, Damanhour, Al-Beheira, Egypt

²Albany College of Pharmacy and Health Sciences, Rensselaer, NY, USA

³University of Jeddah, Jeddah, Makkah, Saudi Arabia

⁴King Abdulaziz University, Jeddah, Saudi Arabia

Corresponding Authors:

Ali H El-Far, Department of Biochemistry, Faculty of Veterinary Medicine, Damanhour University, Damanhour, Al-Beheira 22511, Egypt.
Email: ali.elfar@damanhour.edu.eg

Shaker A. Mousa, Pharmaceutical Research Institute, Albany College of Pharmacy and Health Sciences, Rensselaer, NY 12144, USA.
Email: shaker.mousa@acphs.edu



Cancer is a leading cause of morbidity and mortality worldwide.¹⁴ It is the first or second leading cause of death before the age of 70 years in 112 of 183 countries and ranks third or fourth in a further 23 countries according to estimates from the World Health Organization (WHO) in 2019.¹⁵ Breast cancer has now surpassed lung cancer as the leading cause of global cancer incidence in 2020, with an estimated 2.3 million new cases, representing 11.7% of all cancer cases.¹⁶ Clinically, breast cancer is classified according to its histopathological appearance and expression of hormone receptors and growth factors including the estrogen receptor (ER), the progesterone receptor (PR), and human epidermal growth factor receptor 2 (HER2). ER-positive is the most prevalent type.¹⁷

Colorectal cancer cases were increased by more than 1.9 million new cases and 935 000 deaths in 2020, representing about 1 in 10 cancer cases associated with mortality.¹⁶ For both cancer types, studies have been done to establish curative regimens using either chemotherapeutics, natural products, or combination of both.²

Chemotherapy is a type of cancer treatment that uses 1 or more chemotherapeutic agents.¹⁸ An anthracycline antibiotic, doxorubicin (Dox), is one of the most used cancer drug to treat various types of cancer by inducing cancer senescence.¹⁹ Cellular senescence is an irreversible arrest of growth caused by various harmful stimuli.²⁰ The senescent cells have a larger and flattened cell form and elevation of senescence-associated β -galactosidase (SA- β -gal) activity.^{21,22} In senescence, p53 protein phosphorylation with p21 upregulation was recognized as leading to the arrest of the cell cycle.²³ Many chemotherapy medications at low doses change cancer cells' states and induce senescence features of treated cancer cells.²⁴ Cisplatin and Dox are the first chemotherapeutics reported to induce senescence in tumor cells.^{25,26} Dox is a frequently used chemotherapy in treating numerous cancers and induces cell growth arrest with senescence markers.^{27,28} The senescent cells lose their proliferation, migration, and invasion abilities and develop the senescence-associated secretory phenotype (SASP), wherein the cells secrete high levels of pro-inflammatory mediators.²⁹ Thus senescent cells have tumor-promoting effects on the surrounding microenvironment, where coculture of senescent fibroblasts induced the generation of preneoplasia of prostate epithelial cells.³⁰ A relapse of tumor growth despite Dox-induced senescence and cell cycle arrest of tumors was observed in a mouse xenograft model.²⁷ Also, some cells are still proliferative after Dox treatment; therefore, in the current study, we determined the abilities of TQ and COS to induce apoptosis of proliferative and senescent HCT116 and MCF7 cell lines after Dox treatment.

Materials and Methods

Cell Lines

Human colon HCT116 and breast MCF7 cancer cell lines were purchased from ATCC (Manassas, VA, USA). Each cell line was grown in a recommended medium, McCoy's 5A medium for HCT116 and low glucose Dulbecco's Modified Eagle Medium for MCF7, supplemented with 10% fetal bovine serum and 1% penicillin/streptomycin solution.

Bromodeoxyuridine Incorporation

HCT116 or MCF7 cells were cultured in 12-well plates (3×10^4 per well) and incubated at 37°C in a 5% CO₂ incubator. After 24 hours, cells were treated with bromodeoxyuridine (BrdU, Sigma-Aldrich, MO, USA) at a concentration of 3 μ g/ml. After washing, cells were treated with DAPI (1 μ g/ml) for 10 minutes. The extent of BrdU incorporation in cells was examined using a fluorescence microscope (Nikon, Melville, NY, USA).² BrdU positive cells were counted with ImageJ software (National Institutes of Health, Bethesda, MD, USA).

Senescence-Associated β -Galactosidase Assay

The amounts of SA- β -gal in Sen-HCT116 and Sen-MCF7 cells for 5 days were determined according to the method of Dimri et al.³¹ Cells were examined using the fluorescence microscope after mounting with DAPI.² SA- β -gal positive cells were counted with ImageJ software.

Cell Cycle Analysis

Using a BD Accuri C6 Plus flow cytometer (Becton Dickinson, San Jose, CA, USA), the cell cycle status were analyzed in Dox-treated HCT116 and Dox-treated MCF7 cells.^{2,32}

MTT [3-(4,5-Dimethylthiazol-2-yl)-2,5-Diphenyltetrazolium Bromide] Assay

The IC₅₀ of TQ and COS were determined by seeding HCT116 or MCF7 cells in 12-well plates (3×10^4 per well) and incubated for 24 hours at 37°C in a 5% CO₂ incubator. At day 5 of 100 nM Dox treatment, cells were treated with TQ (0, 5, 10, 25, 50, 60, 75, or 100 μ M dissolved in DMSO) or COS (0, 10, 25, 50, 75, 100, or 200 μ M dissolved in DMSO), incubated for 24 hours, and then treated with MTT reagent (1.25 mg/ml) and incubated for 2 hours. The resulting formazan crystals were dissolved in 1 ml DMSO, and the optical density was determined using a microplate reader at 570 nm.²

Cell Proliferation Assay

HCT116 or MCF7 cells were seeded in 96-well plates (0.5 million cells per well) and were treated with TQ (50 μ M) or COS (30 μ M). At the end of the experiments, the cell cultures were supplemented with MTT reagent and incubated for an additional 4 hours. Then, DMSO (0.1%) was added to the cell culture to dissolve the formazan crystals and incubated for 10 minutes at room temperature. The absorbance rate of the cell cultures was read at 570 nm by using a Microplate Reader (Bio-Rad, Hercules, CA, USA). All the reactions were performed in triplicate. Measured data of cellular proliferation were calculated using viability values of untreated control cells (100%).

Flow Cytometric Assessment

HCT116 or MCF7 cell lines were cultured in T25 flasks (30×10^4 cells per flask) for 24 hours and then treated with 10 ml of TQ (50 μ M) or COS (30 μ M) in each flask for proliferative cells. For Sen-cells, the same counts of cells were cultured and treated with 100 nM of Dox (10 ml) for 5 days, after which 10 ml of TQ (50 μ M) or COS (30 μ M) were added. Treated cells with their corresponding control flasks were trypsinized, washed with PBS, and suspended in 70% ethanol until flow cytometry assessment of senescence (p53 and p21), apoptotic (Bax), and anti-apoptotic (Bcl2) protein markers using a BD Accuri C6 Plus flow cytometer (Becton Dickinson, San Jose, CA, USA). Cells were treated with FITC-conjugated and mouse-raised anti-p53 (Cat # 554298), anti-p21 (Cat # 612236), and anti-Bcl2 (Cat # 340650) produced by Becton Dickinson and anti-Bax (Cat # sc-7480) produced by Santa Cruz Biotechnology (Dallas, TX, USA). Data were analyzed using Accuri C6 software.

Western Blot Analysis

Dox-treated HCT116 and Dox-treated MCF7 cells were lysed and prepared for SDS-PAGE analysis electroblotted to a PVDF membrane. The protein levels of p53 and p21 were quantified and visualized by using anti-p53, anti-p21^{Cip1}, and anti-glyceraldehyde 3-phosphate dehydrogenase (GAPDH) (Santa Cruz, Dallas, TX, USA).^{2,32}

Reverse Transcription Polymerase Chain Reaction (RT-PCR)

HCT116 or MCF7 cell lines, either proliferative or senescent, were cultured in T25 flasks and treated the same way as in the flow cytometry assessment. Total RNA in pelleted cells was extracted using a Total RNA Extraction Kit (iNtRON Biotechnology, Inc., Gyeonggi-do, South Korea). cDNA reverse transcription of the extracted 1 μ g of RNA was performed with a TIANScript RT Kit (Tiangen,

Shanghai, China). RT-PCR was performed with iCycler-iQ Optical System Software version 3.0 A (Bio-Rad, CA, USA). The following primers were used for the quantitative RT-PCR analysis: for caspase 3 (forward): CATGGAAGCGA ATCAATGGACT and reverse: CTGTACCAGACCGAG ATGTCA, and the housekeeping GAPDH forward primer sequence is GAAGGTGAAGGTCGGAGTCA, and the reverse sequence is TTGAGGTCAATGAAGGGGTC.

PCR amplification was done with RealMOD™ Green FAST qPCR Master Mix (S) (Tiangen) using the following conditions: 1 cycle at 95°C for 30 seconds, 40 cycles at 95°C for 5 seconds, 1 cycle at 95°C for 5 seconds. The relative mRNA expression levels of caspase 3 gene were calculated using the comparative (Ct) method.³³

Caspase 3 Activity

Caspase 3 activity was determined using fluorometric assay kits (ThermoFischer Scientific, Hanover Park, IL, USA) according to the manufacturer's protocol. HCT116 or MCF 7 cells were cultured in T25 flasks for 24 hours and then treated with TQ (50 μ M) or COS (30 μ M) in each flask for proliferative cells. For senescent cells, the same counts of cells were cultured and treated with 100 nM of Dox (10 ml) for 5 days, after which TQ (50 μ M) or COS (30 μ M) were added for 24 hours. The treated cells and respective controls were trypsinized and the cell pellet was lysed with cell lysis buffer subjecting to a freeze-thaw cycle for 30 minutes. The lysed pellet was then centrifuged ($10000 \times g$, 4°C, 30 minutes), and protein concentrations were measured with Bradford's reagent (Bio-Rad Laboratories, Inc.), using albumin as a standard. Briefly, 50 μ l of cell protein or the albumin standard was mixed with 200 μ l Bradford reagent and incubated for 15 minutes at room temperature in the dark. The absorbance at 620 nm was measured with a spectrophotometer, and the protein concentration was calculated using a standard. A total of 5 μ l cell lysates (0.5 mg/ml) were added to 195 μ l of buffer containing an Ac-DEVD-7-amino-4-methylcoumarin (AMC)-conjugated substrate for caspase 3. This was followed by 30 minutes incubation at 37°C in the dark. The concentration of the released AMC was calculated from the fluorescence intensity, which was read using a fluorescence plate reader with the excitation and emission wavelengths of 342 and 441 nm, respectively, and using AMC standard to calculate caspase 3 activity. Data were adjusted according to the protein content.

Annexin-V Assay

Apoptosis was analyzed by flow cytometry using annexin V-fluorescein isothiocyanate (annexin-FITC) and propidium iodide (PI) detection kit (BD Biosciences, San Jose, CA, USA). HCT116 or MCF 7 cells were cultured in T25 flasks for 24 hours and then treated with TQ (50 μ M) or

COS (30 μ M) in each flask for proliferative cells. For senescent cells, the same counts of cells were cultured and treated with 100 nM of Dox (10 ml) for 5 days, after which TQ (50 μ M) or COS (30 μ M) were added. Treated cells with their corresponding control flasks were collected and centrifuged at $500 \times g$ for 5 minutes at room temperature. The pellet was rinsed twice with PBS and then resuspended in a proper volume of binding buffer. After addition of 10 μ l of annexin V-FITC followed by gentle mixing incubated for 15 minutes at room temperature in the dark and washed. The fluorescence intensity of FITC was carried on a FACSCalibur™ (Becton Dickinson) instrument, using Cell Quest software.

Statistical Analysis

Statistical analyses were done with GraphPad Prism 5 (San Diego, CA, USA) using 1-way ANOVA (Tukey's Multiple Comparison Test). The IC_{50} values were determined with nonlinear regression using log (inhibitor) versus response-variable slope equation. Data are presented as a mean \pm SD. A value of $P < .05$ was considered statistically significant. All data show the mean results from at least 3 independent experiments.

Results

Senescence Markers

Changes in the senescence markers of HCT116 cells treated with 100 nM of Dox are illustrated in Figure 1a and b. HCT116 treated with Dox for 5 consecutive days exhibited significant increases ($P < .001$) in SA- β -gal positive cells at day 1 (day 1 after Dox treatment of HCT116, Dox 1) and day 5 (day 5 after Dox treatment of HCT116, Dox 5) in comparison with Dox 0 (control, Dox-untreated HCT116). Also, on day 5, SA- β -gal positive cells were significantly increased ($P < .001$) compared with Dox 1.

BrdU incorporation in Sen-HCT116 cells significantly decreased ($P < .001$) at days 2 and 5 in comparison with Dox 0 (Figure 1c and d). Incorporation of BrdU in Sen-HCT116 cells was significantly decreased ($P < .001$) on day 5 compared with day 2.

The percentages of SA- β -gal positive cells indicate the extent of accumulation SA- β -gal in senescent cells, leading to enlargement of the senescent cells. The percentages of BrdU positive cells at Dox 5 of the senescent cells are low due to the low cell division.

The cell cycle of Dox-treated HCT116 was arrested; concomitantly, the percentages of cells in G2/M phase were increased (Figure 1e).

Protein expression levels of p53 (Figure 1f and g) and p21 (Figure 1h and i) of Sen-HCT116 were significantly ($P < .05$) increased at day 1 of Dox treatment of HCT116 compared with control.

Sen-MCF7 exhibited the exact extent of senescent markers such as Sen-HCT116 regarding SA- β -gal positivity and BrdU incorporation in cells (Figure 2a–d). Also, the cell cycle was arrested with increment in G2/M phase percentages (Figure 2e). The expression of p53 monitored with flow cytometry was significantly increased at day 1 ($P < .05$) and day 5 ($P < .01$) compared with Dox 0 (Figure 2f and g). Also, the p21 expression was significantly ($P < .01$) increased at day 1 and 5 compared with Dox 0 (Figure 2h and i). Also, the protein expression of p53 and p21 were increased in Sen-HCT116 and Sen-MCF7 at day 1 and 5 as evidenced by Western blot analyses that illustrated in Figure 1j and Figure 2j, respectively.

IC_{50} and Cell Proliferation of Thymoquinone and Costunolide

The IC_{50} of TQ against HCT116 is $64.15 \pm 2.80 \mu$ M (Figure 3a) and $36.95 \pm 6.09 \mu$ M against MCF7 (Figure 3b), and the IC_{50} of COS against HCT116 is $32.08 \pm 0.86 \mu$ M (Figure 3c) and $40.84 \pm 1.89 \mu$ M against MCF7 (Figure 3d).

HCT116 cells treated with either 50 μ M of TQ or 30 μ M of COS exhibited significant ($P < .001$) decreases in cell proliferation compared with untreated HCT116. Also, MCF7 cell proliferation was significantly decreased in response to TQ ($P < .001$) and COS ($P < .01$) treatment by the same doses compared with untreated MCF7 (Figure 3e).

Caspase 3 mRNA Expression

Relative expression folds of caspase 3 mRNA of Sen-HCT116 treated with Dox for 5 days then treated with 50 μ M of TQ for 24 hours (HCT116 + Dox5 + TQ) were significantly increased ($P < .001$) compared with control (untreated, proliferative HCT116), Dox5, and HCT116 + TQ (untreated, proliferative HCT116 then treated with 50 μ M of TQ) (Figure 4a).

Regarding MCF7, the relative expression of caspase 3 mRNA was significantly ($P < .01$) increased in MCF7 + TQ (untreated, proliferative MCF7 then treated with 50 μ M of TQ for 24 hours) and MCF7 + Dox5 + TQ (Sen-MCF7 with Dox for 5 days and then treated with 50 μ M of TQ for 24 hours) compared with control (untreated, proliferative MCF7). Cells in the MCF7 + Dox5 + TQ group exhibited significant increases ($P < .05$) in caspase 3 expression in comparison with Dox5, while Dox5 expressed significant decreases ($P < .05$) in caspase 3 gene compared with MCF7 + TQ (Figure 4b).

In the same manner, 30 μ M of COS significantly increased ($P < .01$) the relative expression fold change levels of caspase 3 mRNA in Sen-HCT116 in comparison with control (untreated, proliferative HCT116), Dox5, and HCT116 + TQ (Figure 4c).

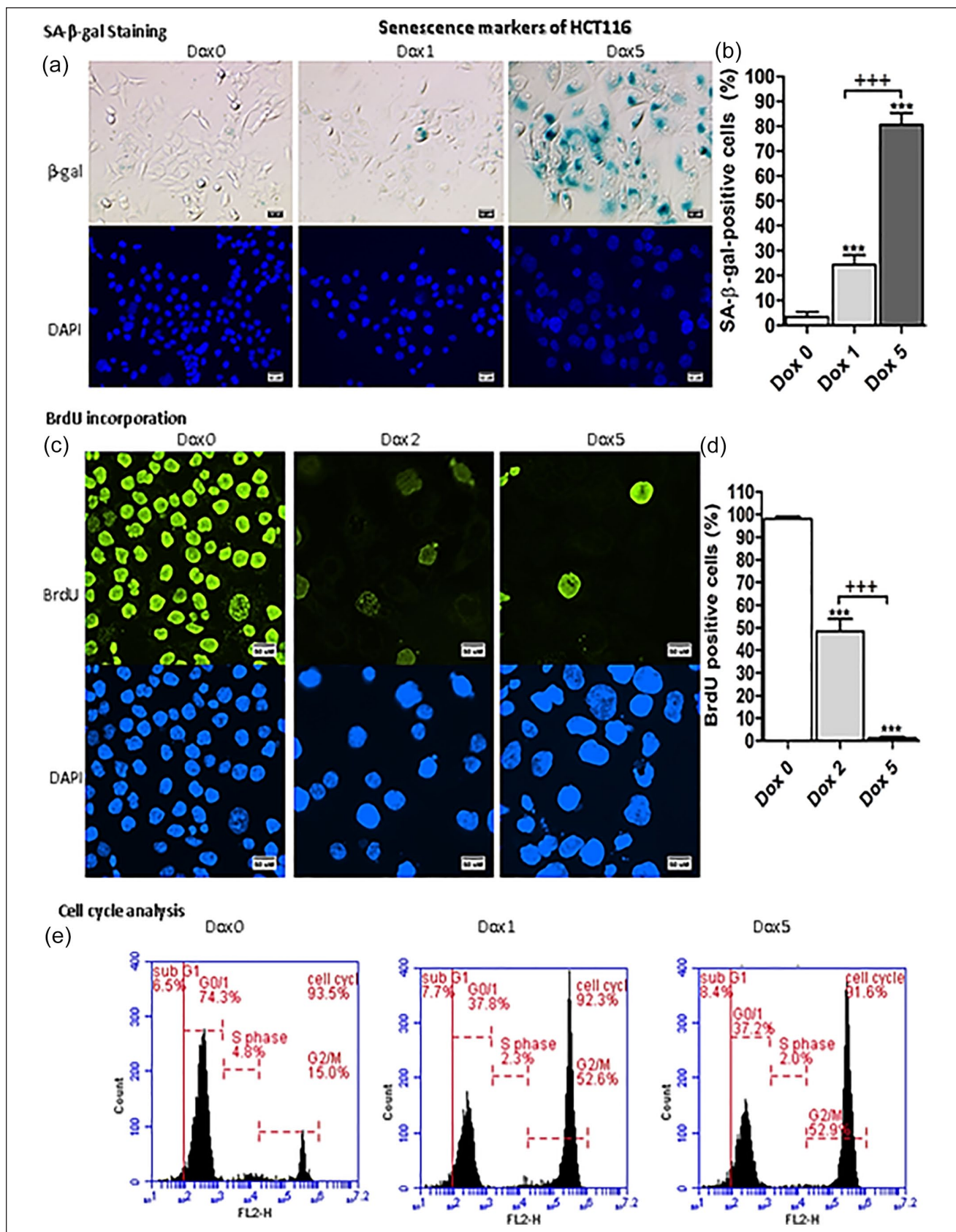


Figure I. (continued)

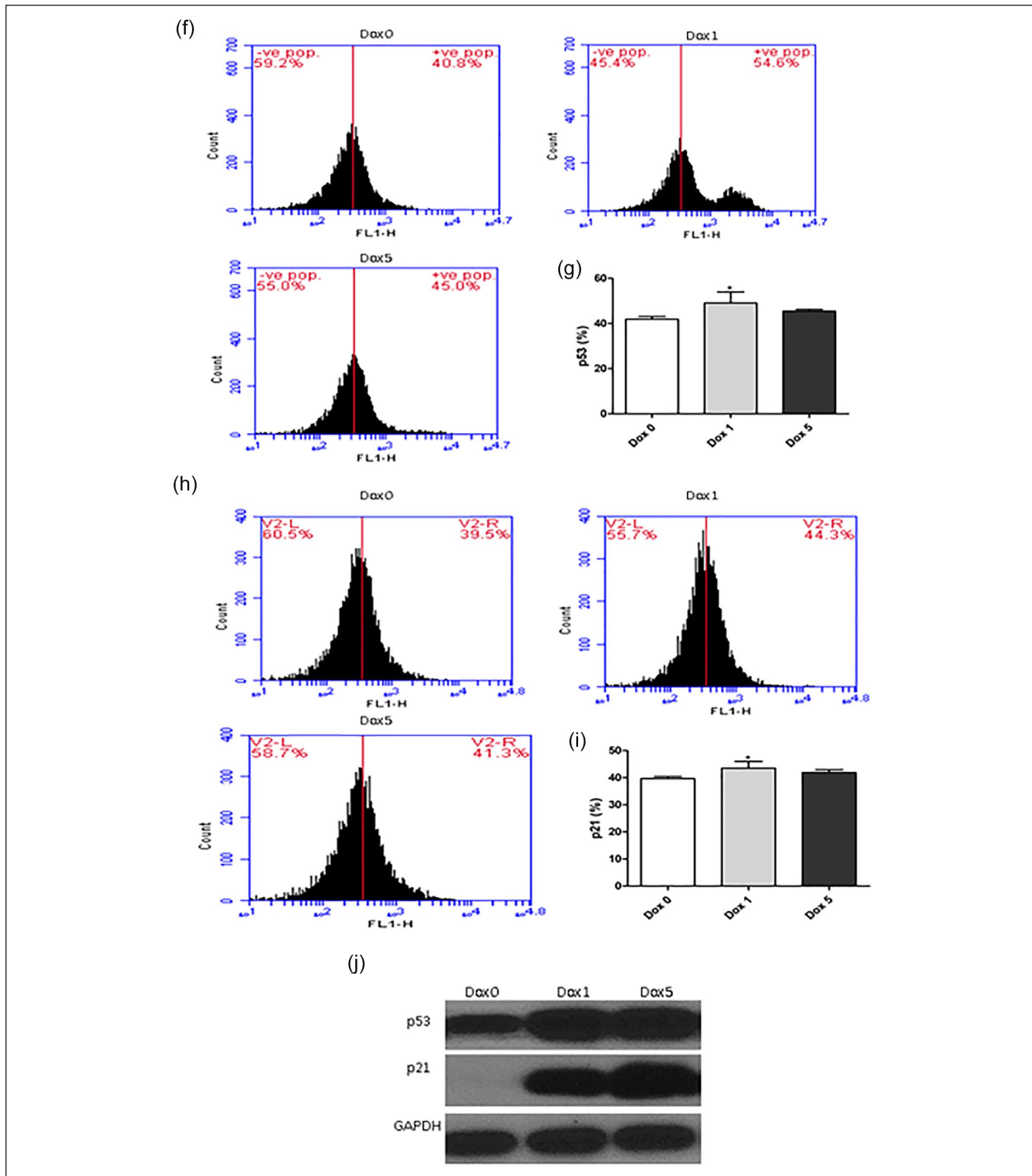


Figure 1. Senescence markers of Sen-HCT116. (a) SA- β -gal-positive cells of Sen-HCT116 cells. The scale bar is 50 μ m. (b) SA- β -gal-positive cells percentages. (c) BrdU incorporation for Sen-HCT116 cells. Magnification 200 \times . The scale bar is 50 μ m. (d) BrdU positive cells percentages. (e) representative cell cycle analysis. (f) p53 protein expressions by flow cytometry of Sen-HCT116 cells. (g) p53 protein expression percentages. (h) p21 protein expressions by flow cytometry of Sen-HCT116 cells. (i) p21 protein expression percentages. (j) Western blot analysis of p53 and p21. The data were analyzed with 1-way ANOVA (Tukey's Multiple Comparison Test). Error bars represent mean \pm SD. * P < .05 and *** P < .001 versus Day 0 (control). +++ P < .001 versus Dax 1 (SA- β -gal) and Dax 2 (BrdU). Dax 0 refers to untreated cells. Dax 1 refers to day 1 after Dox treatment. Dax 5 refers to day 5 after Dox treatment. All assays were done in triplicate at least.

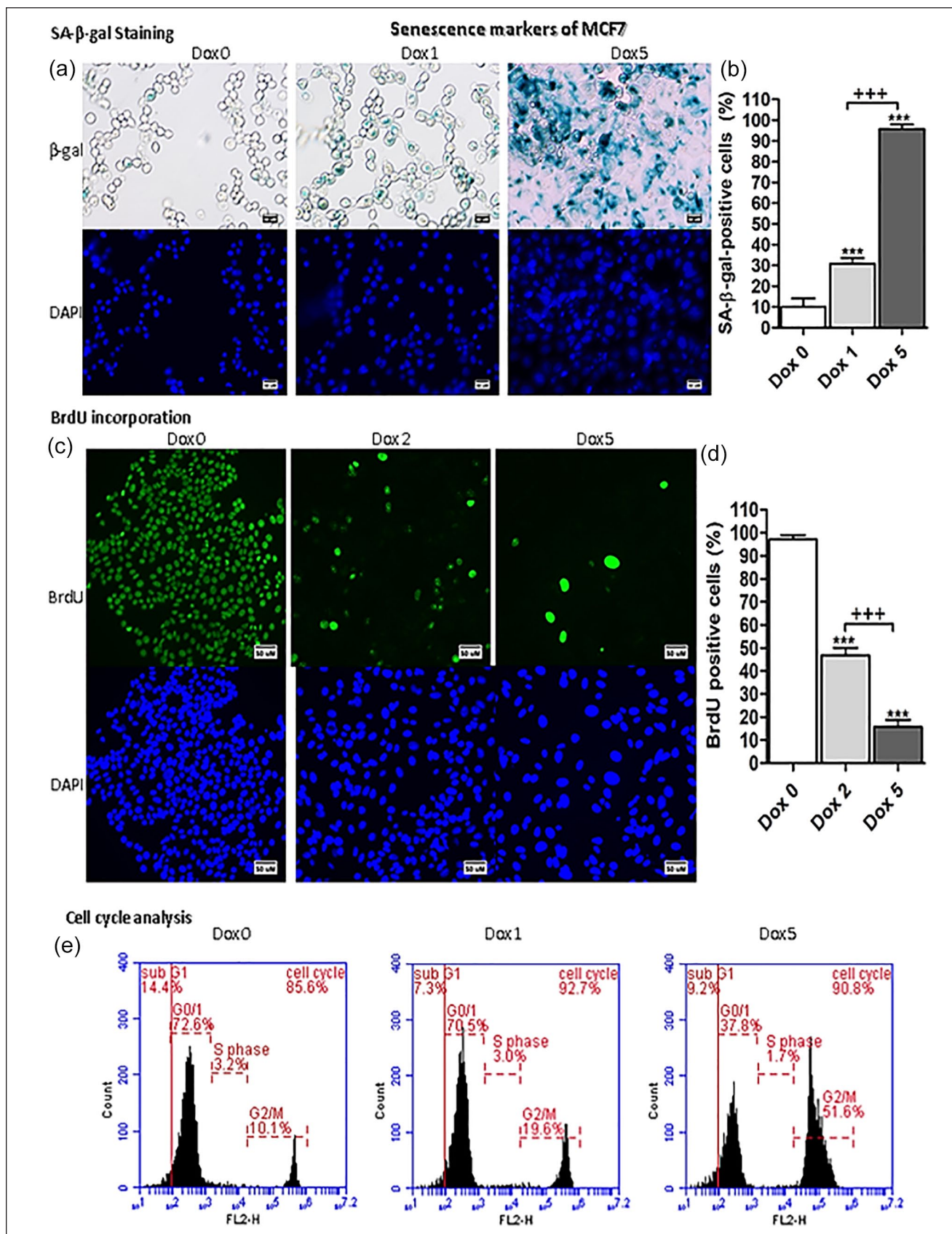


Figure 2. (continued)

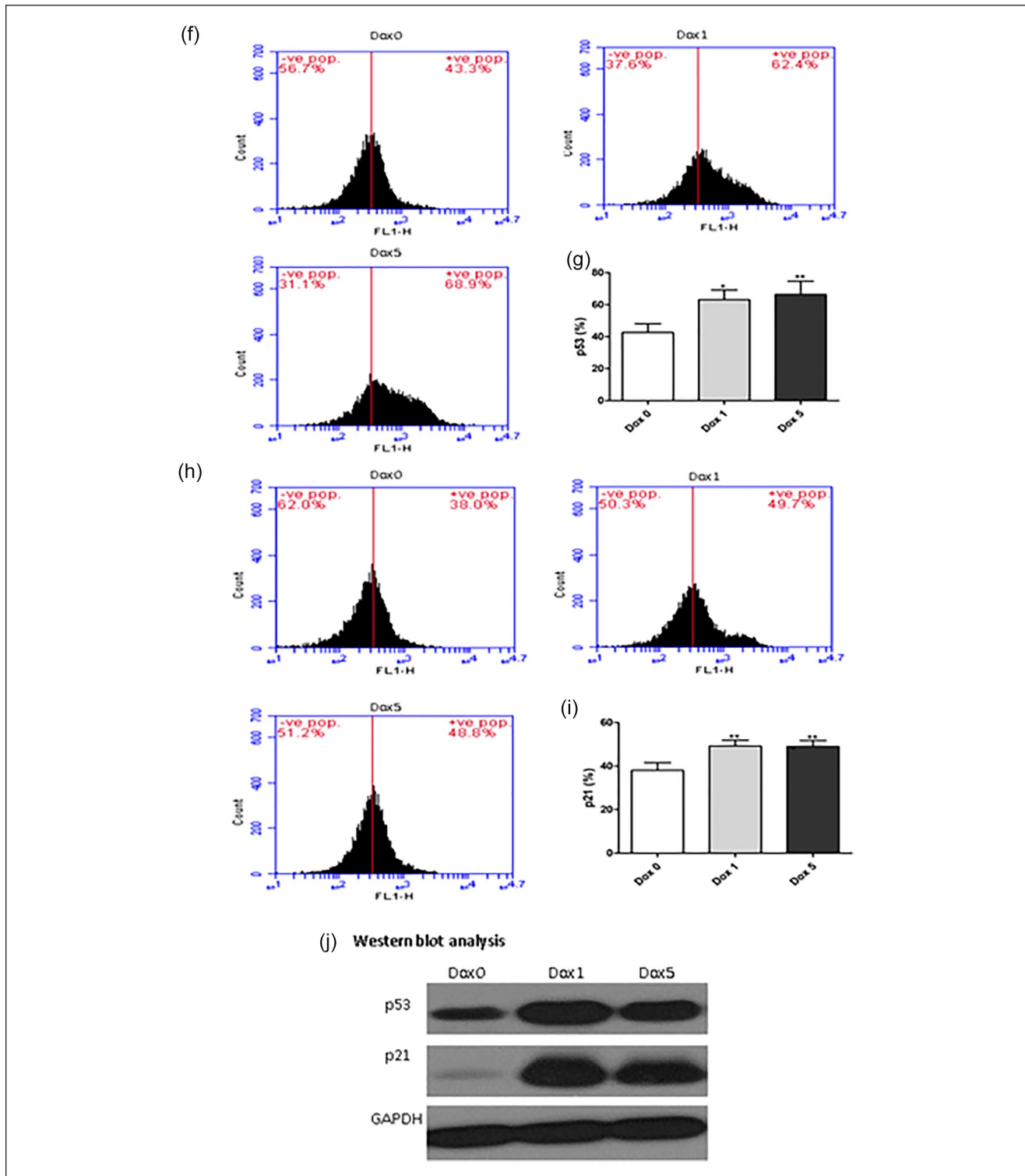


Figure 2. Senescence markers of Sen-MCF7. (a) SA- β -gal-positive cells of Sen-MCF7 cells. The scale bar is 50 μ m. (b) SA- β -gal-positive cells percentages. (c) BrdU incorporation for Sen-MCF7 cells. Magnification 200 \times . The scale bar is 50 μ m. (d) BrdU positive cells percentages. (e) representative cell cycle analysis. (f) p53 protein expressions by flow cytometry of Sen-HCT116 cells. (g) p53 protein expression percentages. (h) p21 protein expressions by flow cytometry of Sen-HCT116 cells. (i) p21 protein expression percentages. (j) Western blot analysis of p53 and p21. The data were analyzed with 1-way ANOVA (Tukey's Multiple Comparison Test). Error bars represent mean \pm SD. * P < .05, ** P < .01, and *** P < .001 versus Day 0 (control). +++ P < .001 versus Dox 1 (SA- β -gal) and Dox 2 (BrdU). Dox 0 refers to untreated cells. Dox 1 refers to day 1 after Dox treatment. Dox 5 refers to day 5 after Dox treatment. All assays were done in triplicate at least.

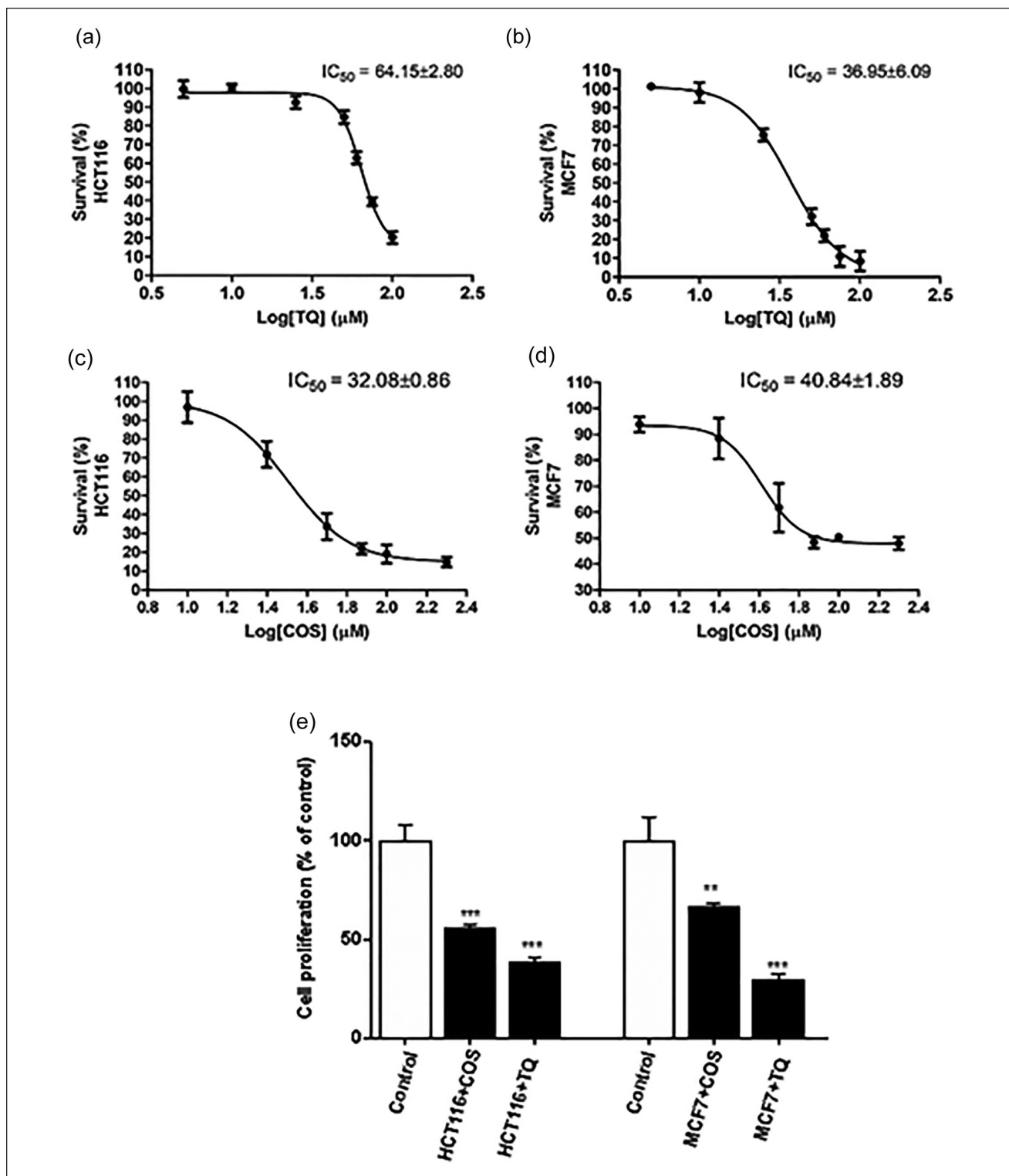


Figure 3. IC_{50} values of thymoquinone (TQ) against (a) HCT116 and (b) MCF7 and of costunolide (COS) against (c) HCT116 and (d) MCF7. (e) Cell proliferation percentages of HCT116 and MCF7 treated with TQ (50 μM) and COS (30 μM). Error bars represent mean \pm SD. ** $P < .01$ and *** $P < .001$ versus control. Control refers to proliferative-untreated HCT116 or -untreated MCF7. HCT116 + TQ refers to HCT116 treated with 50 μM TQ for 24 hours. MCF7 + TQ refers to HCT116 treated with 50 μM TQ for 24 hours. HCT116 + COS refers to HCT116 treated with 30 μM COS for 24 hours. MCF7 + COS refers to HCT116 treated with 30 μM COS for 24 hours. All assays were done in triplicate at least.

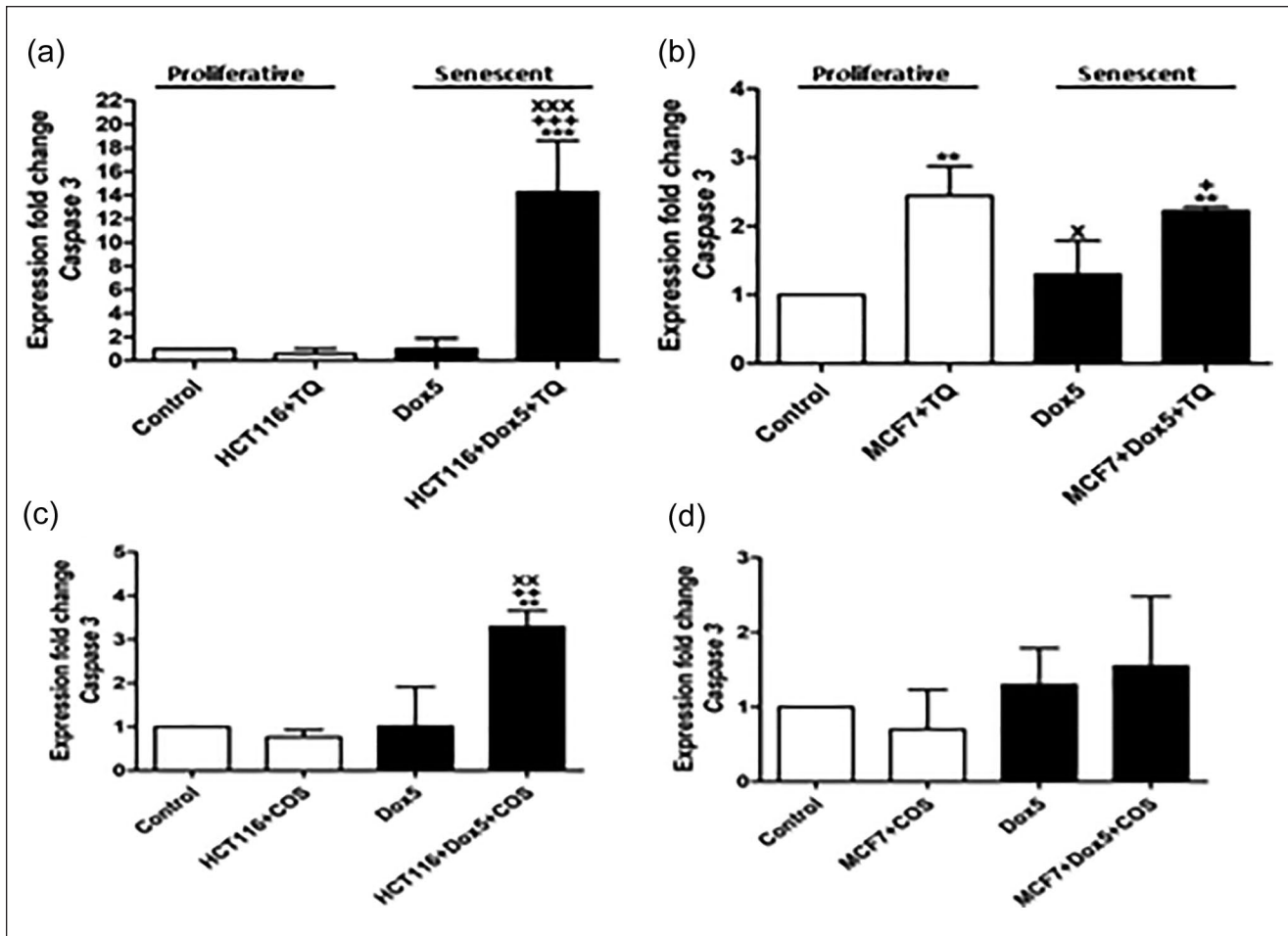


Figure 4. Caspase 3 mRNA expression. (a) Caspase 3 mRNA relative fold changes in HCT116 and Sen-HCT116 treated with thymoquinone (TQ, 50 μ M). (b) Caspase 3 mRNA relative fold changes in MCF7 and Sen-MCF7 treated with thymoquinone (TQ, 50 μ M). (c) Caspase 3 mRNA relative fold changes in HCT116 and Sen-HCT116 treated with costunolide (COS, 30 μ M). (d) Caspase 3 mRNA relative fold changes in MCF7 and Sen-MCF7 treated with costunolide (COS, 30 μ M). Error bars represent mean \pm SD. ** $P < .01$ and *** $P < .001$ versus control. * $P < .05$, ** $P < .01$, and *** $P < .001$ versus Dox5. * $P < .05$, ** $P < .01$, and *** $P < .001$ versus HCT116 + COS or MCF7 + COS. Control refers to proliferative-untreated HCT116 or -untreated MCF7. HCT116 + TQ refers to HCT116 treated with 50 μ M TQ for 24 hours. MCF7 + TQ refers to HCT116 treated with 50 μ M TQ for 24 hours. HCT116 + COS refers to HCT116 treated with 30 μ M COS for 24 hours. MCF7 + COS refers to HCT116 treated with 30 μ M COS for 24 hours. Dox5 refers to Sen-HCT116 or Sen-MCF7 with 100 nM Dox for 5 days. HCT116 + Dox5 + COS refers to Sen-HCT116 with 100 nM Dox for 5 days then treated with 30 μ M COS for 24 hours. MCF7 + Dox5 + COS refers to Sen-MCF7 with 100 nM Dox for 5 days then treated with 30 μ M COS for 24 hours. All assays were done in triplicate at least.

Caspase Activity

Caspase 3 activities of HCT116 ($P < .01$) and Sen-HCT116 ($P < .001$) treated with TQ (50 μ M) were significantly increased compared with control. Furthermore, TQ-treated MCF7 ($P < .05$) and Sen-MCF7 ($P < .001$) had significantly increased caspase 3 activities compared with control (Figure 5a). Its levels in Sen-HCT116 and Sen-MCF7 were also significantly ($P < .001$) increased compared with HCT116 + TQ and MCF7 + TQ, respectively. Nearly similar results have been stated when HCT116, Sen-HCT116,

MCF7, and Sen-MCF7 were treated with 30 μ M of COS except MCF7 + COS exhibited more increased significant ($P < .01$) caspase 3 activity compared with untreated MCF7 (Figure 5b).

Bax and Bcl2 Proteins

Bax protein levels of HCT116, either proliferative or senescent, are presented in Figures 6a and b. Bax levels were significantly decreased ($P < .05$) in Dox5, while significantly increased ($P < .01$) in HCT116 + Dox5 + TQ

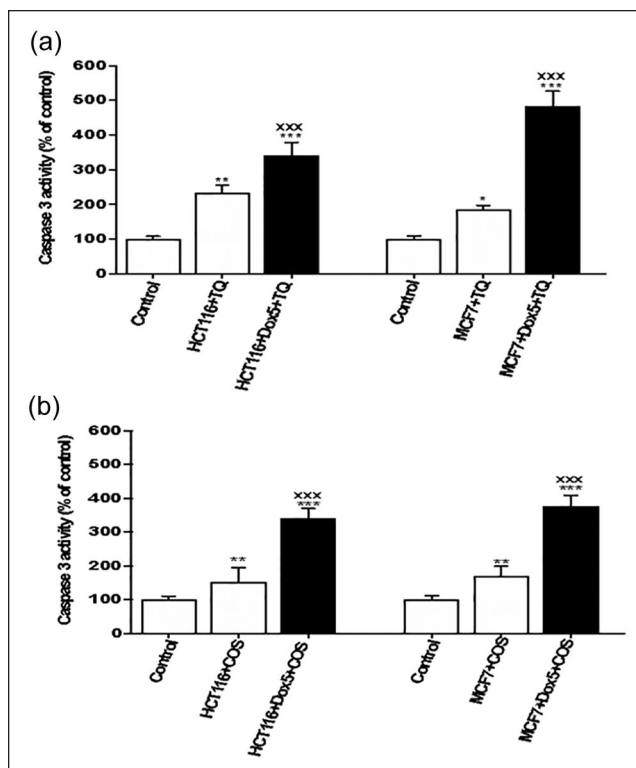


Figure 5. Caspase 3 activity. (a) Caspase 3 activity in HCT116 and MCF7 treated with thymoquinone (TQ, 50 μ M). (b) Caspase 3 activity in HCT116 and MCF7 treated with costunolide (COS, 30 μ M). Error bars represent mean \pm SD. * $P < .05$, ** $P < .01$, and *** $P < .001$ versus control, xxx $P < .001$ versus HCT116 + COS or MCF7 + COS. Control refers to proliferative-untreated HCT116 or -untreated MCF7. HCT116 + TQ refers to HCT116 treated with 50 μ M TQ for 24 hours. MCF7 + TQ refers to HCT116 treated with 50 μ M TQ for 24 hours. HCT116 + COS refers to HCT116 treated with 30 μ M COS for 24 hours. MCF7 + COS refers to HCT116 treated with 30 μ M COS for 24 hours. Control refers to proliferative-untreated HCT116 or -untreated MCF7. HCT116 + TQ refers to HCT116 treated with 50 μ M TQ for 24 hours. MCF7 + TQ refers to HCT116 treated with 50 μ M TQ for 24 hours. Dox5 refers to Sen-HCT116 or Sen-MCF7 with 100 nM Dox for 5 days. HCT116 + Dox5 + TQ refers to Sen-HCT116 with 100 nM Dox for 5 days, then treated with 50 μ M TQ for 24 hours. MCF7 + Dox5 + TQ refers to Sen-MCF7 with 100 nM Dox for 5 days then treated with 50 μ M TQ for 24 hours. TQ, thymoquinone; COS, costunolide. All assays were done in triplicate at least.

compared with control. Also, its expression was significantly increased in HCT116 + Dox5 + TQ compared with Dox5 and HCT116 + TQ.

Bcl2 protein levels were significantly increased in Dox5 ($P < .001$) and HCT116 + Dox5 + TQ ($P < .01$) compared with control. In the HCT116 + Dox5 + TQ cells, Bcl2 protein levels were significantly increased ($P < .01$) compared with HCT116 + TQ and significantly decreased ($P < .01$) compared with Dox5 (Figure 6c and d).

Figure 6e and f show significant increases ($P < .01$) in Bax levels in MCF7 + TQ, Dox5, and MCF7 + Dox5 + TQ compared with control.

In comparison with control MCF7, Bcl2 protein levels were significantly decreased ($P < .01$) in MCF7 + TQ and significantly increased in Dox5 ($P < .001$) and MCF7 + Dox5 + TQ ($P < .01$) as shown in Figure 6g and h. Also, Bcl2 levels in Dox5 and MCF7 + Dox5 + TQ were significantly increased ($P < .001$) in comparison with MCF7 + TQ. MCF7 + Dox5 + TQ exhibited significant reduction ($P < .001$) in Bcl2 levels compared with Dox5.

Data in Figure 7 represent the effect of COS (30 μ M) on proliferative HCT116, proliferative MCF7, Sen-HCT116, and Sen-MCF7. Bax levels were significantly decreased ($P < .05$) in Dox5 and increased ($P < .001$) in HCT116 + Dox5 + COS compared with control. In the HCT116 + Dox5 + COS, Bax levels were significantly increased ($P < .001$) compared with Dox5 and HCT116 + COS (Figure 7a and b). In the same cell line, Bcl2 levels were significantly increased ($P < .001$) in Dox5 and HCT116 + Dox5 + COS compared with control and HCT116 + COS (Figure 7c and d).

In MCF7, the Bax levels were significantly increased ($P < .05$) in Dox5 compared with MCF7 + COS (Figure 7e and f). Bcl2 levels were significantly increased ($P < .001$) in Dox5 and MCF7 + Dox5 + COS compared with control and MCF7 + COS. The MCF7 + Dox5 + COS exhibited significant decreases ($P < .001$) in Bcl2 in comparison with Dox5.

When the data of each cell line was compared with their corresponding control of either proliferative or senescent cells (Table 1), TQ (50 μ M) significantly increased ($P < .001$) Bax and significantly decreased ($P < 0.001$) Bcl2 in Sen-HCT116 and consequently increased Bax/Bcl2 ratio in Sen-HCT116 (1.72). TQ at the same concentration significantly increased ($P < .001$) Bax and significantly decreased ($P < .001$) Bcl2 in MCF7 + TQ compared with control, while in Sen-MCF7, TQ significantly decreases ($P < .001$) Bcl2 compared with Dox5. Therefore, the Bax/Bcl2 ratio in proliferative and Sen-MCF7 was increased by 1.69 and 1.33, respectively, compared with their corresponding control. From these results, we can conclude that TQ (50 μ M) induced apoptosis in both proliferative and Sen-MCF7, especially in proliferative MCF7 that exhibited a greater Bax/Bcl2 ratio than Sen-MCF7.

By the same approach, 30 μ M of COS significantly increased ($P < .001$) Bax in HCT116 + Dox5 + COS and significantly decreased ($P < .001$) Bcl2 of MCF7 + Dox5 + COS compared with corresponding Dox5 controls (Table 2). Consequently, the Bax/Bcl2 ratios were increased in Sen-HCT116 (1.86) and Sen-MCF7 (1.14) compared with proliferative cells.

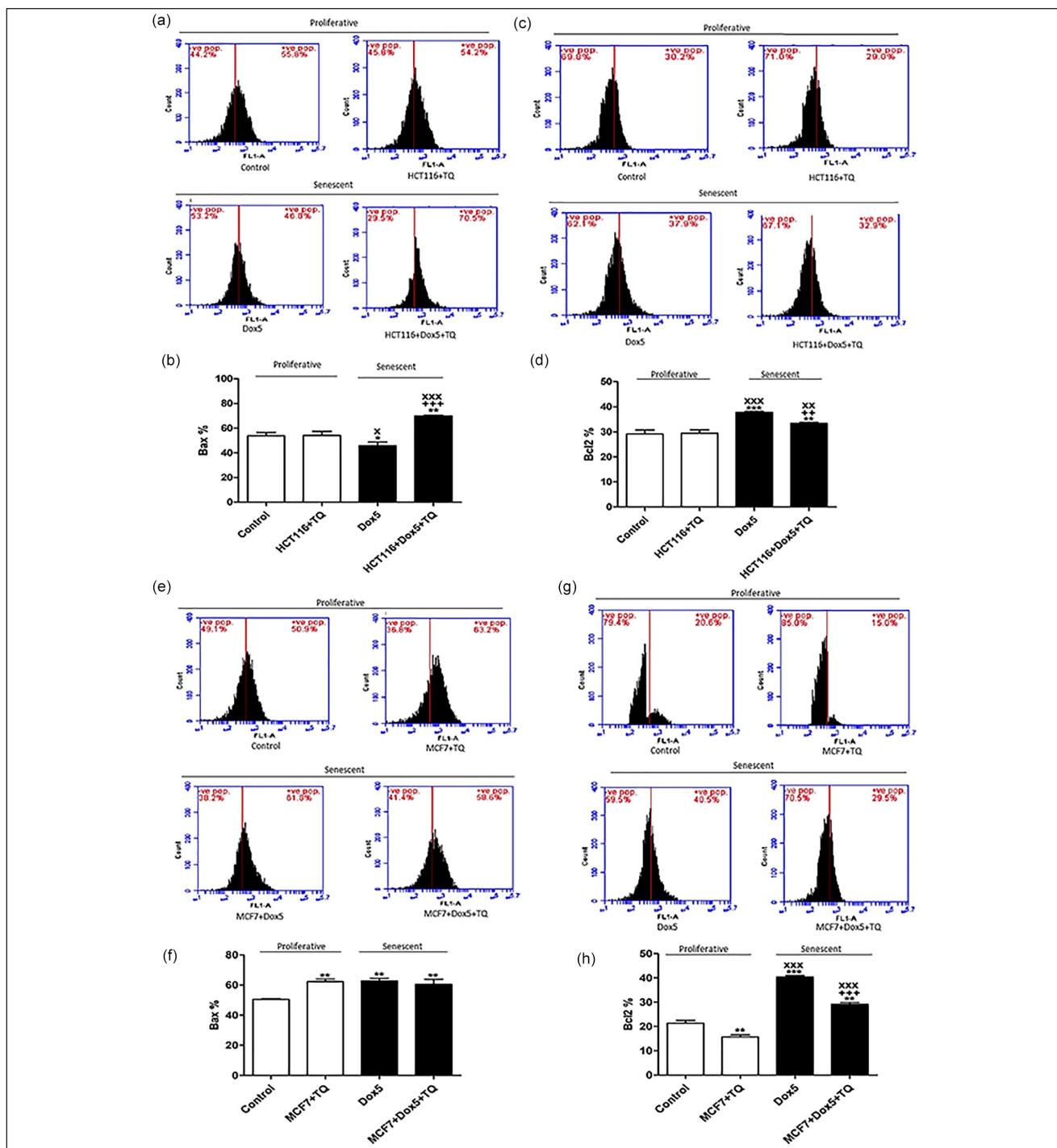


Figure 6. Bax and Bcl2 protein expressions of proliferative HCT116, Sen-HCT116, and proliferative MCF7, Sen-MCF7 cells by flow cytometry. (a) Bcl2-associated X protein (Bax) protein levels of proliferative and Sen-HCT116. (b) Percentages of Bax protein levels of proliferative and Sen-HCT116. (c) B-cell lymphoma 2 (Bcl2) protein levels of proliferative and Sen-HCT116. (d) Percentages of Bcl2 protein levels of proliferative and Sen-HCT116. (e) Bax protein levels of proliferative and Sen-MCF7. (f) Percentages of Bax protein levels of proliferative and Sen-MCF7. (g) Bcl2 protein levels of proliferative and Sen-MCF7. (h) Percentages of Bcl2 protein levels of proliferative and Sen-MCF7. The data were analyzed with 1-way ANOVA (Tukey's Multiple Comparison Test). Error bars represent mean \pm SD. * $P < .05$, ** $P < .01$, and *** $P < .001$ versus control. ++ $P < .01$ and +++ $P < .001$ versus Dox5. * $P < .05$, ** $P < .01$, and *** $P < .001$ versus HCT116 + TQ or MCF7 + TQ. Control refers to proliferative-untreated HCT116 or -untreated MCF7. HCT116 + TQ refers to HCT116 treated with 50 μ M TQ for 24 hours. MCF7 + TQ refers to HCT116 treated with 50 μ M TQ for 24 hours. Dox5 refers to Sen-HCT116 or Sen-MCF7 with 100 nM Dox for 5 days. HCT116 + Dox5 + TQ refers to Sen-HCT116 with 100 nM Dox for 5 days, then treated with 50 μ M TQ for 24 hours. MCF7 + Dox5 + TQ refers to Sen-MCF7 with 100 nM Dox for 5 days then treated with 50 μ M TQ for 24 hours. TQ, thymoquinone. All assays were done in triplicate at least.

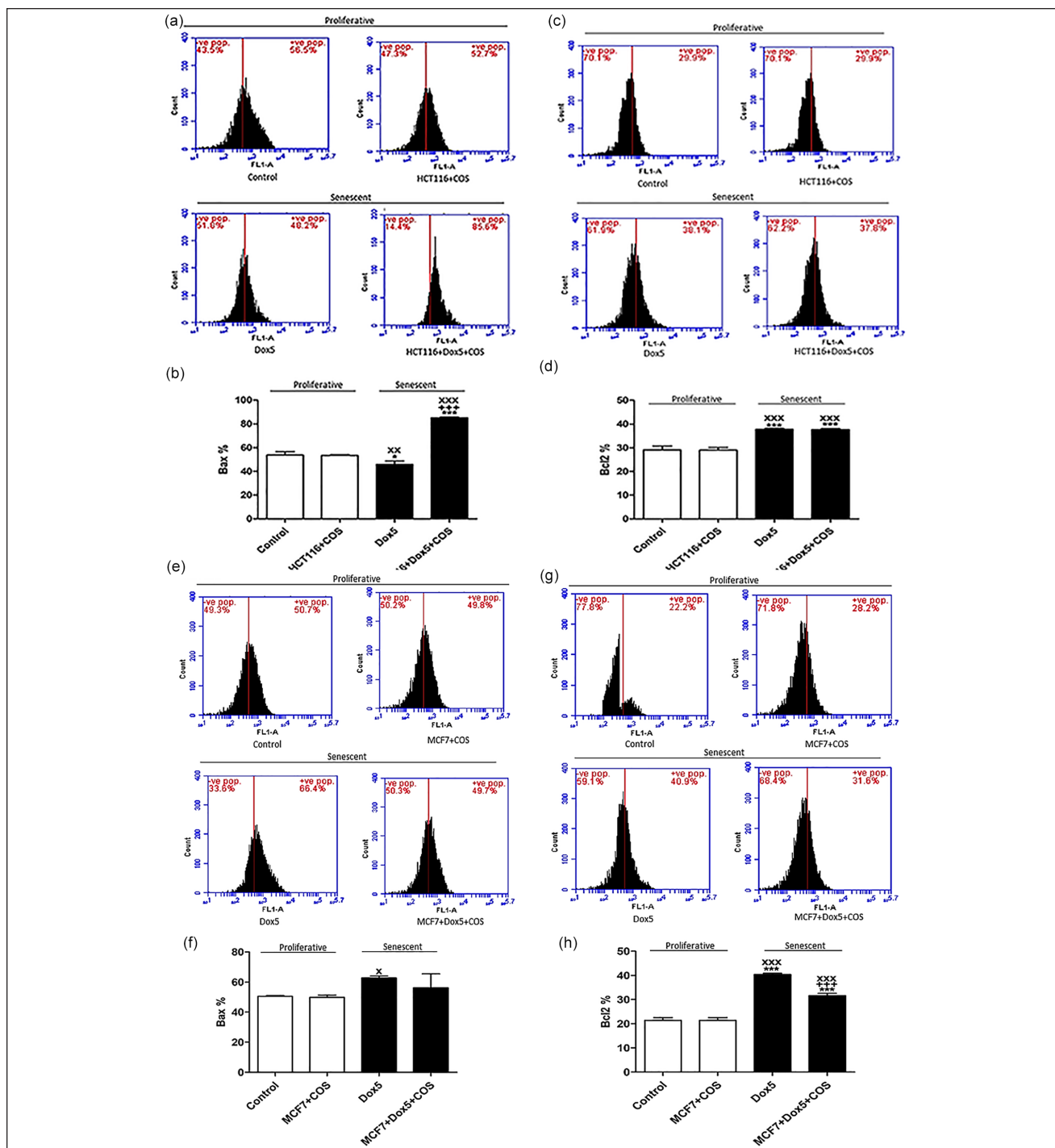


Figure 7. Bax and Bcl2 protein expressions of proliferative HCT116, Sen-HCT116, and proliferative MCF7, Sen-MCF7 cells by flow cytometry. (a) Bcl2-associated X protein (Bax) protein levels of proliferative and Sen-HCT116. (b) Percentages of Bax protein levels of proliferative and Sen-HCT116. (c) B-cell lymphoma 2 (Bcl2) protein levels of proliferative and Sen-HCT116. (d) Percentages of Bcl2 protein levels of proliferative and Sen-HCT116. (E) Bax protein levels of proliferative and Sen-MCF7. (f) Percentages of Bax protein levels of proliferative and Sen-MCF7. (g) Bcl2 protein levels of proliferative and Sen-MCF7. (h) Percentages of Bcl2 protein levels of proliferative and Sen-MCF7. The data were analyzed with 1-way ANOVA (Tukey's Multiple Comparison Test). Error bars represent mean \pm SD. * $P < .05$ and ** $P < .001$ versus control. +++ $P < .001$ versus Dox5. * $P < .05$, ** $P < .01$, and *** $P < .001$ versus HCT116 + COS or MCF7 + COS. Control refers to proliferative-untreated HCT116 or -untreated MCF7. HCT116 + COS refers to HCT116 treated with 30 μ M COS for 24 hours. MCF7 + COS refers to HCT116 treated with 30 μ M COS for 24 hours. Dox5 refers to Sen-HCT116 or Sen-MCF7 with 100 nM Dox for 5 days. HCT116 + Dox5 + COS refers to Sen-HCT116 with 100 nM Dox for 5 days then treated with 30 μ M COS for 24 hours. MCF7 + Dox5 + COS refers to Sen-MCF7 with 100 nM Dox for 5 days then treated with 30 μ M COS for 24 hours. COS, costunolide. All assays were done in triplicate at least.

Table 1. Percentages of Bcl2-associated X protein (Bax) and B-cell lymphoma 2 (Bcl2) protein levels to their corresponding control of either proliferative or senescent cells (HCT116 and MCF7) treated with thymoquinone (TQ).

	HCT116				MCF7			
	Proliferative		Senescence		Proliferative		Senescence	
	Control	HCT116 + TQ	Dox5	HCT116 + Dox5 + TQ	Control	MCF7 + TQ	Dox5	MCF7 + Dox5 + TQ
Bax	100	100.5 ± 3.3	100	152.4 ± 0.6***	100	123.4 ± 1.7***	100	96.3 ± 3.4
Bcl2	100	101.4 ± 1.3	100	88.4 ± 0.5***	100	73.1 ± 0.9***	100	72.3 ± 0.7***
Bax/Bcl2 ratio	1	0.99	1	1.72	1	1.69	1	1.33

Mean ± SD. *** $P < .001$ versus control or Dox5. Control refers to proliferative-untreated HCT116 or -untreated MCF7. HCT116 + TQ refers to HCT116 treated with 50 μ M TQ for 24 hours. MCF7 + TQ refers to HCT116 treated with 50 μ M TQ for 24 hours. Dox5 refers to Sen-HCT116 or Sen-MCF7 with 100 nM Dox for 5 days. HCT116 + Dox5 + TQ refers to Sen-HCT116 with 100 nM Dox for 5 days, then treated with 50 μ M TQ for 24 hours. MCF7 + Dox5 + TQ refers to Sen-MCF7 with 100 nM Dox for 5 days then treated with 50 μ M TQ for 24 hours.

Table 2. Percentages of Bcl2-associated X protein (Bax) and B-cell lymphoma 2 (Bcl2) protein levels to their corresponding control of either proliferative or senescent cells (HCT116 and MCF7) treated with costunolide (COS).

	HCT116				MCF7			
	Proliferative		Senescence		Proliferative		Senescence	
	Control	HCT116 + COS	Dox5	HCT116 + Dox5 + COS	Control	MCF7 + COS	Dox5	MCF7 + Dox5 + COS
Bax	100	99.4 ± 0.7	100	185.7 ± 0.5***	100	98.8 ± 1.4	100	89.7 ± 9.2
Bcl2	100	99.5 ± 1.1	100	99.8 ± 0.3	100	100 ± 1.1	100	78.4 ± 0.9***
Bax/Bcl2 ratio	1	1	1	1.86	1	0.99	1	1.14

Mean ± SD. *** $P < .001$ versus control or Dox5. Control refers to proliferative-untreated HCT116 or -untreated MCF7. HCT116 + COS refers to HCT116 treated with 30 μ M COS for 24 hours. MCF7 + COS refers to HCT116 treated with 30 μ M COS for 24 hours. Dox5 refers to Sen-HCT116 or Sen-MCF7 with 100 nM Dox for 5 days. HCT116 + Dox5 + COS refers to Sen-HCT116 with 100 nM Dox for 5 days then treated with 30 μ M COS for 24 hours. MCF7 + Dox5 + COS refers to Sen-MCF7 with 100 nM Dox for 5 days then treated with 30 μ M COS for 24 hours.

Apoptotic Effect of Thymoquinone and Costunolide

Fluorescence-activated cell sorting analysis was conducted to investigate the apoptosis induced by TQ or COS or in combination with Dox. Proliferative HCT116 cells ($P < .01$) and Sen-HCT116 (HCT116 + Dox5 + TQ) cells ($P < .001$) treated with TQ (50 μ M) showed a significant increase in annexin positive cells compared with untreated control. Further, Sen-HCT116 cells treated COS (30 μ M) exhibited a significant ($P < .001$) increase in annexin positive cells compared with control (Figure 8).

A significant increase in percentage of Annexin positive cells was observed in MCF7 cells and Sen-MCF7 treated with TQ (50 μ M) or COS (30 μ M) compared with untreated MCF7 cells (Figure 9).

Discussion

Markers of senescence such as SA- β -gal and protein levels of p53 and p21 were significantly increased in the Sen-HCT116 and Sen-MCF7 in addition to

significant decreases in BrdU incorporation. The same results were found when HCT116 or MCF7 cell lines were treated with 100 nM of Dox.^{2,34,35} HCT116 exposed to 50 nM,³⁶⁻³⁸ 75 nM,³⁹ 100 nM,^{2,32,38,40-42} and 200 nM⁴³ for 1 to 4 days exhibited the features of senescence. Higher doses of Dox induced senescence in HCT116 by doses of 1 μ M for 2 hours⁴⁴ and 500 nM for 4 hours.⁴⁵ In the same manner, MCF7 expressed the senescence feature when subjected to different levels of Dox such as 38 nM,⁴⁶ 50 nM,^{36,47} 75 nM,^{39,48} 100 nM,^{2,34,35} and 500 nM⁴⁹ for 1 to 5 days. Also, high doses of Dox 1 μ M⁵⁰ and 10 μ M⁵¹ for 2 hours were used to induce senescence in a short time. Researchers used either low Dox doses for long periods or high dose for a maximum of 2 hours to enhance the senescence process before induction of cancer cell apoptosis by Dox.

In the studies as mentioned earlier, Dox induced upregulation of p53, especially the phospho-p53 (Ser15) that consequently upregulated p21,² which induced cell cycle arrest through inhibition of cyclin E/cyclin-dependent kinase 2 (CDK2) and cyclin-dependent kinase (CDK1) activities.⁵² Besides, SA- β -gal accumulated in the

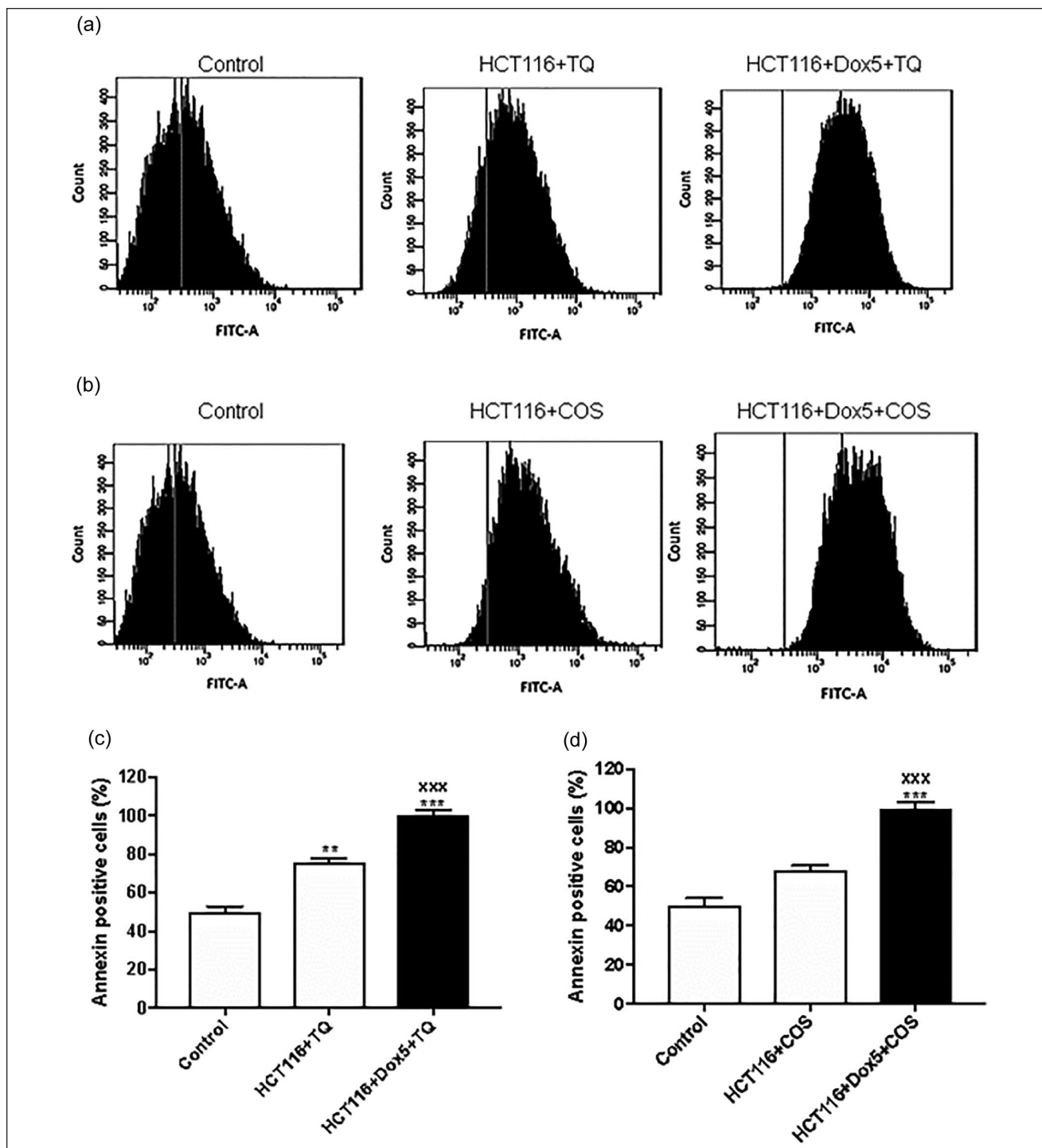


Figure 8. Annexin-V of proliferative HCT116 and Sen-HCT116 cells by flow cytometry. (a) Histogram of HCT116 and Sen-HCT116 treated with 50 μ M thymoquinone (TQ) for 24 hours. (b) Histogram of HCT116 and Sen-HCT116 treated with 30 μ M costunolide (COS) for 24 hours. (c) Percentages of annexin-v positive cells of HCT116 and Sen-HCT116 treated with 50 μ M TQ for 24 hours. (d) Percentages of annexin-v positive cells of HCT116 and Sen-HCT116 treated with 30 μ M COS for 24 hours. The data were analyzed with 1-way ANOVA (Tukey's Multiple Comparison Test). Error bars represent mean \pm SD. ** P < .01 and *** P < .001 versus control. *** P < .001 versus HCT116 + TQ or HCT116 + COS. Control refers to proliferative-untreated HCT116. HCT116 + TQ refers to HCT116 treated with 50 μ M TQ for 24 hours. HCT116 + COS refers to HCT116 treated with 30 μ M COS for 24 hours. HCT116 + Dox5 + TQ refers to Sen-HCT116 with 100 nM Dox for 5 days, then treated with 50 μ M TQ for 24 hours. HCT116 + Dox5 + COS refers to Sen-HCT116 with 100 nM Dox for 5 days then treated with 30 μ M COS for 24 hours. TQ, thymoquinone. COS, costunolide. All assays were done in triplicate at least.

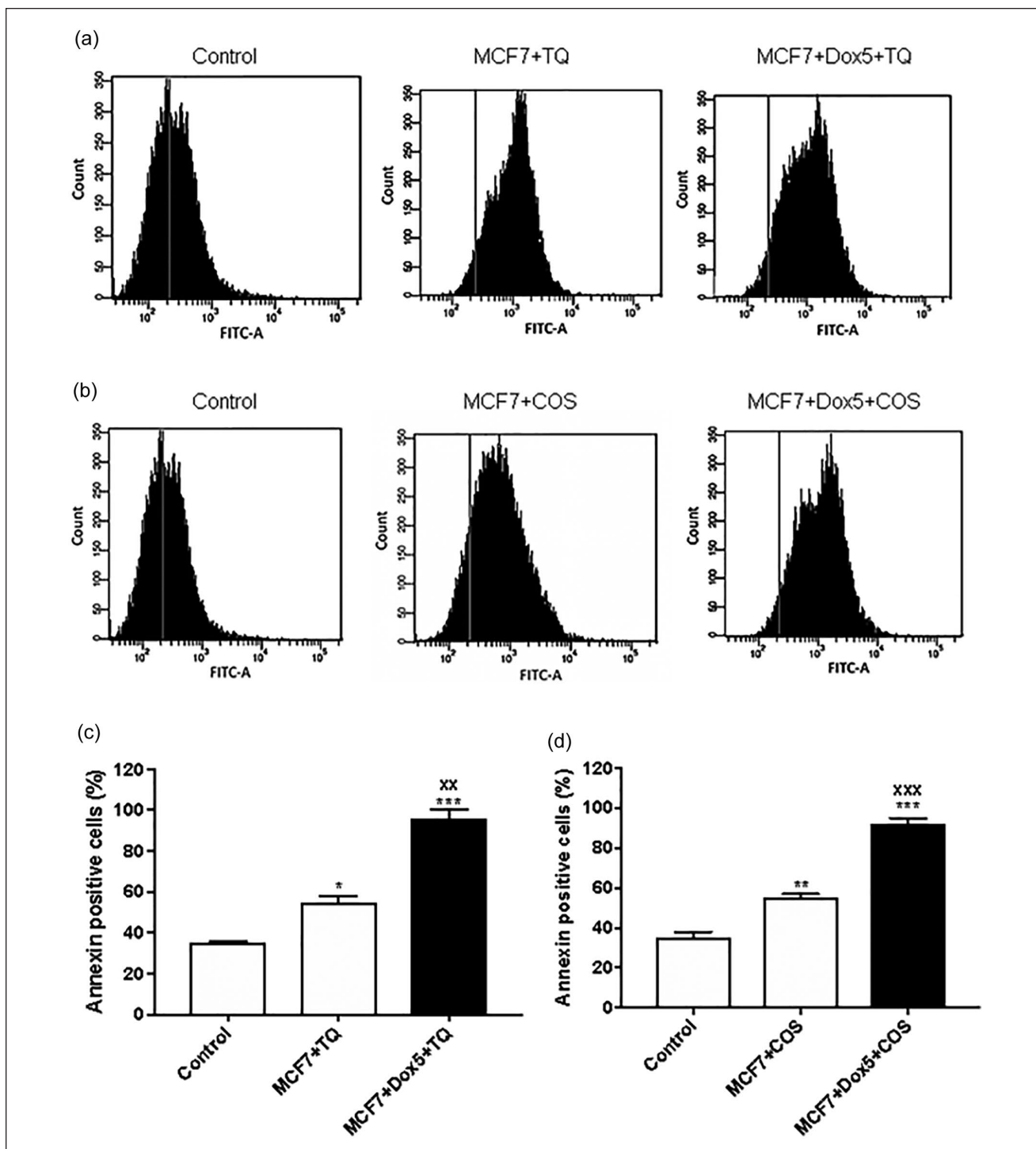


Figure 9. Annexin-V of proliferative MCF7, Sen-MCF7 cells by flow cytometry. (a) Histogram of MCF7 and Sen-MCF7 treated with 50 μ M thymoquinone (TQ) for 24 hours. (b) Histogram of MCF7 and Sen-MCF7 treated with 30 μ M costunolide (COS) for 24 hours. (c) Percentages of annexin-v positive cells of MCF7 and Sen-MCF7 treated with 50 μ M TQ for 24 hours. (d) Percentages of annexin-v positive cells of MCF7 and Sen-MCF7 treated with 30 μ M COS for 24 hours. The data were analyzed with 1-way ANOVA (Tukey's Multiple Comparison Test). Error bars represent mean \pm SD. * P < .05, ** P < .01, and *** P < .001 versus control. ** p < .01 and *** p < .001 versus MCF7 + TQ or MCF7 + COS. Control refers to proliferative-untreated MCF7. MCF7 + TQ refers to MCF7 treated with 50 μ M TQ for 24 hours. MCF7 + COS refers to MCF7 treated with 30 μ M COS for 24 hours. MCF7 + Dox5 + TQ refers to Sen-MCF7 with 100 nM Dox for 5 days, then treated with 50 μ M TQ for 24 hours. MCF7 + Dox5 + COS refers to Sen-MCF7 with 100 nM Dox for 5 days then treated with 30 μ M COS for 24 hours. TQ, thymoquinone. COS, costunolide. All assays were done in triplicate at least.

Dox-treated cancer cells, leading to enlargement of cancer cells, and senescent HCT116 cells try to escape from senescence by polyploidization.^{2,24}

Results of the present study revealed that TQ exhibited IC_{50} against HCT116 and MCF7, $64.15 \pm 2.80 \mu\text{M}$ and $36.95 \pm 6.09 \mu\text{M}$, respectively, while COS is $32.08 \pm 0.86 \mu\text{M}$ for HCT116 and $40.84 \pm 1.89 \mu\text{M}$ for MCF7. Similarly, Fröhlich et al⁵³ stated that TQ has IC_{50} of 50.1 ± 6.1 for HCT116 and 42.0 ± 8.5 for MCF7. Roy and Manikkam¹³ determined the IC_{50} of COS against MCF7 by $40 \mu\text{M}$.

Caspase 3 is a major executing protein in cellular exposure to cytotoxic medications, radiation therapy, or immunotherapy during proteolytic degradation. It is also used as a marker for cancer treatment effectiveness.⁵⁴ In the current study, TQ significantly increased caspase 3 expression and activity in proliferative HCT116, proliferative MCF7, Sen-HCT116, and Sen-MCF7 treated with TQ. Numerous published studies revealed significant upregulation in caspase 3 in p53-null myeloblastic leukemia (HL-60),⁵⁵ human lung (LNM35),⁵⁶ human osteosarcoma (MG63),⁵⁷ HCT116,⁵⁸ and MCF7⁵⁹ cancer cell lines treated with TQ. Also, COS induced upregulation and activation of caspase 3 in multi-drug-resistant ovarian cancer (OAW42)⁶⁰ and human gastric (BGC-823)⁶¹ proliferative cancer cell lines.

Bax is a pro-apoptotic protein responsible for causing cell death, and Bcl2 is an anti-apoptotic protein that regulates the mitochondrial membrane function and protects cells from apoptosis.⁶² Both Bax and Bcl2 are regulated by the tumor-suppressor protein p53.⁶³ Therefore, an increased Bax/Bcl2 ratio is a factor in predisposing apoptosis.^{64,65} In the current study, Bax levels were significantly increased in HCT116 + Dox5 + TQ compared with their control senescent (Dox5), and Bcl2 levels were significantly decreased. These data indicate the sensitivity of Sen-HCT116 to TQ-induced apoptosis compared with proliferative HCT116. Also, MCF7 + Dox5 + TQ exhibited significant decreases compared with Dox5 and MCF7 + TQ that favored apoptosis Sen-MCF7. The sensitivity of Sen-HCT116 and Sen-MCF7 to TQ compared with their corresponding proliferative cells has been stated in our previous study.² Also, COS induced increases in Bax/Bcl2 ratio in HCT116 + Dox5 + TQ and MCF7 + Dox5 + TQ compared with their corresponding Dox5 cells. These results indicate the sensitivity of both Sen-HCT116 and Sen-MCF7 to COS compared with their corresponding proliferative cells.

Conclusion

Dox is a commonly used chemotherapeutic agent for cancer treatment and induces cellular senescence of both HCT116 and MCF7 cell lines. To prevent the relapse of these senescent cells to proliferative cells and induce apoptosis of cancer cells that still are proliferative even after Dox treatment,

we intervened with TQ and COS to rapidly eliminate the senescent cells and induce apoptosis of proliferative cancer cell lines. Both TQ and COS induced more apoptosis of Sen-HCT116 and Sen-MCF7 than their proliferative cells by different extents and cell specificity. We suggest that future in vivo and clinical trials include either TQ or COS in the Dox treatment schedule of cancer.

Acknowledgments

We appreciate Kelly Keating (Medical editor and writer) from the Pharmaceutical Research Institute, Rensselaer, NY, USA for her editorial assistance.

Author Contributions

Conceptualization: Ali H. El-Far, Kavitha Godugu, Ahmed E. Noreldin, Amna A. Saddiq, Omar A. Almaghrabi, and Soad K. Al Jaouni; Data curation: Ali H. El-Far, Amna A. Saddiq, Soad K. Al Jaouni, and Shaker A. Mousa; Formal analysis: Ali H. El-Far and Ahmed E. Noreldin; Funding acquisition: Amna A. Saddiq, Omar A. Almaghrabi, Soad K. Al Jaouni, and Shaker A. Mousa; Investigation: Ali H. El-Far, Kavitha Godugu, and Ahmed E. Noreldin; Methodology: Ali H. El-Far; Project administration: Ali H. El-Far; Resources: Ali H. El-Far, Kavitha Godugu, Ahmed E. Noreldin, and Shaker A. Mousa; Software: Ali H. El-Far, Ahmed E. Noreldin, and Shaker A. Mousa; Supervision: Ali H. El-Far, Amna A. Saddiq, Omar A. Almaghrabi, Soad K. Al Jaouni, and Shaker A. Mousa; Validation: Ali H. El-Far; Visualization: Ali H. El-Far; Writing—original draft: Ali H. El-Far; Writing—review and editing: Ali H. El-Far, Kavitha Godugu, Ahmed E. Noreldin, Amna A. Saddiq, Omar A. Almaghrabi, Soad K. Al Jaouni, and Shaker A. Mousa.

Declaration of Conflicting Interests

The author(s) declared no potential conflicts of interest with respect to the research, authorship, and/or publication of this article.

Funding

The author(s) disclosed receipt of the following financial support for the research, authorship, and/or publication of this article: The work was carried out with financial support from the Deputyship for Research and Innovation, Ministry of Education in Saudi Arabia for funding this research work through the project number MoE-IF-G-20-02.

ORCID iD

Ali H El-Far  <https://orcid.org/0000-0001-9721-4360>

References

1. El-Far AH. Thymoquinone anticancer discovery: possible mechanisms. *Curr Drug Discov Technol*. 2015;12:80-89. doi: 10.2174/1570163812666150716111821
2. El-Far AH, Darwish NHE, Mousa SA. Senescent colon and breast cancer cells induced by doxorubicin exhibit

- enhanced sensitivity to curcumin, caffeine, and thymoquinone. *Integr Cancer Ther.* 2020;19:1534735419901160. doi:10.1177/1534735419901160
3. Gali-Muhtasib H, Kuester D, Mawrin C, et al. Thymoquinone triggers inactivation of the stress response pathway sensor CHEK1 and contributes to apoptosis in colorectal cancer cells. *Cancer Res.* 2008;68:5609-5618. doi:10.1158/0008-5472.CAN-08-0884
 4. Atta MS, El-Far AH, Farrag FA, Abdel-Daim MM, Al Jaouni SK, Mousa SA. Thymoquinone attenuates cardiomyopathy in streptozotocin-treated diabetic rats. *Oxid Med Cell Longev.* 2018;2018:1-10. doi:10.1155/2018/7845681
 5. El-Far AH, Al Jaouni SK, Li W, Mousa SA. Protective roles of thymoquinone nanoformulations: potential nanonutraceuticals in human diseases. *Nutrients.* 2018;10:1369. doi:10.3390/nu10101369
 6. Atta MS, Almadaly EA, El-Far AH, et al. Thymoquinone defeats diabetes-induced testicular damage in rats targeting antioxidant, inflammatory and aromatase expression. *Int J Mol Sci.* 2017;18:919. doi:10.3390/ijms18050919
 7. Gali-Muhtasib H, Diab-Assaf M, Boltze C, et al. Thymoquinone extracted from black seed triggers apoptotic cell death in human colorectal cancer cells via a p53-dependent mechanism. *Int J Oncol.* 2004;25:857-866. doi:10.3892/ijo.25.4.857
 8. Dastjerdi MN, Mehdiabady EM, Iranpour FG, Bahramian H. Effect of thymoquinone on P53 gene expression and consequence apoptosis in breast cancer cell line. *Int J Prev Med.* 2016;7:66. doi:10.4103/2008-7802.180412
 9. Woo CC, Hsu A, Kumar AP, Sethi G, Tan KHB. Thymoquinone inhibits tumor growth and induces apoptosis in a breast cancer xenograft mouse model: the role of p38 MAPK and ROS. *PLoS One.* 2013;8:e75356. doi:10.1371/journal.pone.0075356
 10. Kim YE, Choi HC, Nam G, Choi BY. Costunolide promotes the proliferation of human hair follicle dermal papilla cells and induces hair growth in C57BL/6 mice. *J Cosmet Dermatol.* 2019;18:414-421. doi:10.1111/jocd.12674
 11. Kim DY, Choi BY. Costunolide—a bioactive sesquiterpene lactone with diverse therapeutic potential. *Int J Mol Sci.* 2019;20:2926. doi:10.3390/ijms20122926
 12. Hua P, Zhang G, Zhang Y, et al. Costunolide induces G1/S phase arrest and activates mitochondrial-mediated apoptotic pathways in SK-MES 1 human lung squamous carcinoma cells. *Oncol Lett.* 2016;11:2780-2786. doi:10.3892/ol.2016.4295
 13. Roy A, Manikkam R. Cytotoxic impact of costunolide isolated from *Costus speciosus* on breast cancer via differential regulation of cell cycle – an in-vitro and in-silico approach. *Phyther Res.* 2015;29:1532-1539. doi:10.1002/ptr.5408
 14. Bray F, Laversanne M, Weiderpass E, Soerjomataram I. The ever-increasing importance of cancer as a leading cause of premature death worldwide. *Cancer.* June 2021;cncr.33587. doi:10.1002/cncr.33587
 15. World Health Organization (WHO). Global health estimates 2020: deaths by cause, age, sex, by country and by region, 2000-2019. WHO. Accessed June 19, 2021. <https://www.who.int/data/gho/data/themes/mortality-and-global-health-estimates/ghe-leading-causes-of-death>.
 16. Sung H, Ferlay J, Siegel RL, et al. Global Cancer statistics 2020: GLOBOCAN estimates of incidence and mortality worldwide for 36 cancers in 185 countries. *CA Cancer J Clin.* 2021;71:209-249. doi:10.3322/caac.21660
 17. Glass AG, Hoover RN. Rising incidence of breast cancer: relationship to stage and receptor status. *J Natl Cancer Inst.* 1990;82:693-696. doi:10.1093/jnci/82.8.693
 18. Johnstone RW, Ruefli AA, Lowe SW. Apoptosis: a link between cancer genetics and chemotherapy. *Cell.* 2002;108:153-164. doi:10.1016/S0092-8674(02)00625-6
 19. Rivankar S. An overview of doxorubicin formulations in cancer therapy. *J Cancer Res Ther.* 2014;10:853. doi:10.4103/0973-1482.139267
 20. Wang AS, Dreesen O. Biomarkers of cellular senescence and skin aging. *Front Genet.* 2018;9:247. doi:10.3389/fgene.2018.00247
 21. Debacq-Chainiaux F, Erusalimsky JD, Campisi J, Toussaint O. Protocols to detect senescence-associated beta-galactosidase (SA- β gal) activity, a biomarker of senescent cells in culture and in vivo. *Nat Protoc.* 2009;4:1798-1806. doi:10.1038/nprot.2009.191
 22. Chen W, Kang J, Xia J, et al. p53-related apoptosis resistance and tumor suppression activity in UVB-induced premature senescent human skin fibroblasts. *Int J Mol Med.* 2008;21:645-653. doi:10.3892/ijmm.21.5.645
 23. Qian Y, Chen X. Senescence regulation by the p53 protein family. *Methods Mol Biol.* 2013;965:37-61. doi:10.1007/978-1-62703-239-1_3
 24. Mosieniak G, Sliwinska MA, Alster O, et al. Polyploidy formation in doxorubicin-treated cancer cells can favor escape from senescence. *Neoplasia.* 2015;17:882-893. doi:10.1016/j.neo.2015.11.008
 25. Wang X, Wong SCH, Pan J, et al. Evidence of cisplatin-induced senescent-like growth arrest in nasopharyngeal carcinoma cells. *Cancer Res.* 1998;58:5019-5022. Accessed July 9, 2020. <https://pubmed.ncbi.nlm.nih.gov/9823301/>.
 26. Chang BD, Broude E V., Dokmanovic M, et al. A senescence-like phenotype distinguishes tumor cells that undergo terminal proliferation arrest after exposure to anticancer agents. *Cancer Res.* 1999;59:3761-3767.
 27. Demaria M, O'Leary MN, Chang J, et al. Cellular senescence promotes adverse effects of chemotherapy and cancer relapse. *Cancer Discov.* 2017;7:165-176. doi:10.1158/2159-8290.CD-16-0241
 28. Tacar O, Srimornsak P, Dass CR. Doxorubicin: an update on anticancer molecular action, toxicity and novel drug delivery systems. *J Pharm Pharmacol.* 2013;65:157-170. doi:10.1111/j.2042-7158.2012.01567.x
 29. Milczarek M. The premature senescence in breast cancer treatment strategy. *Cancers (Basel).* 2020;12:1815. doi:10.3390/cancers12071815
 30. Bavik C, Coleman I, Dean JP, Knudsen B, Plymate S, Nelson PS. The gene expression program of prostate fibroblast senescence modulates neoplastic epithelial cell proliferation through paracrine mechanisms. *Cancer Res.* 2006;66:794-802. doi:10.1158/0008-5472.CAN-05-1716
 31. Dimri GP, Lee X, Basile G, et al. A biomarker that identifies senescent human cells in culture and in aging skin in vivo. *Proc Natl Acad Sci USA.* 1995;92:9363-9367. Accessed December 16, 2018. <http://www.ncbi.nlm.nih.gov/pubmed/7568133>.

32. Sliwinska MA, Mosieniak G, Wolanin K, et al. Induction of senescence with doxorubicin leads to increased genomic instability of HCT116 cells. *Mech Ageing Dev.* 2009;130:24-32. doi:10.1016/j.mad.2008.04.011
33. Schmittgen TD, Livak KJ. Analyzing real-time PCR data by the comparative CT method. *Nat Protoc.* 2008;3:1101-1108. doi:10.1038/nprot.2008.73
34. Taylor JR, Lehmann BD, Chappell WH, Abrams SL, Steelman LS, McCubrey JA. Cooperative effects of Akt-1 and Raf-1 on the induction of cellular senescence in doxorubicin or tamoxifen treated breast cancer cells. *Oncotarget.* 2011;2:610-626. doi:10.18632/oncotarget.315
35. Basu A, Pal D, Blaydes R. Differential effects of protein kinase C-eta on apoptosis versus senescence. *Cell Signal.* 2019;55:1-7. doi:10.1016/j.cellsig.2018.12.003
36. Shao AW, Sun H, Geng Y, et al. Belaf1 is an important NF- κ B signaling transducer and C/EBP β regulator in DNA damage-induced senescence. *Cell Death Differ.* 2016;23:865-875. doi:10.1038/cdd.2015.150
37. Chang BD, Xuan Y, Broude EV, et al. Role of p53 and p21(waf1/cip1) in senescence-like terminal proliferation arrest induced in human tumor cells by chemotherapeutic drugs. *Oncogene.* 1999;18:4808-4818. doi:10.1038/sj.onc.1203078
38. Drummond CJ, Finlay GJ, Broome L, Marshall ES, Richardson E, Baguley BC. Action of SN 28049, a new DNA binding topoisomerase II-directed antitumour drug: comparison with doxorubicin and etoposide. *Invest New Drugs.* 2011;29:1102-1110. doi:10.1007/s10637-010-9473-8
39. Di X, Bright AT, Bellott R, et al. A chemotherapy-associated senescence bystander effect in breast cancer cells. *Cancer Biol Ther.* 2008;7:682-690. doi:10.4161/cbt.7.6.5861
40. Strzeszewska A, Alster O, Mosieniak G, Ciolko A, Sikora E. Insight into the role of PIKK family members and NF- κ B in DNA damage-induced senescence and senescence-associated secretory phenotype of colon cancer cells. *Cell Death Dis.* 2018;9:44. doi:10.1038/s41419-017-0069-5
41. Tong Y, Zhao W, Zhou C, Wawrowsky K, Melmed S. PTTG1 Attenuates drug-induced cellular senescence. *PLoS One.* 2011;6:e23754. doi:10.1371/journal.pone.0023754
42. Was H, Barszcz K, Czarnańska J, et al. Bafilomycin A1 triggers proliferative potential of senescent cancer cells in vitro and in NOD/SCID mice. *Oncotarget.* 2017;8:9303-9322. doi:10.18632/oncotarget.14066
43. Chang BD, Swift ME, Shen M, Fang J, Broude E V., Roninson IB. Molecular determinants of terminal growth arrest induced in tumor cells by a chemotherapeutic agent. *Proc Natl Acad Sci USA.* 2002;99:389-394. doi:10.1073/pnas.012602599
44. Saleh T, Tyutyunyk-Massey L, Murray GF, et al. Tumor cell escape from therapy-induced senescence. *Biochem Pharmacol.* 2019;162:202-212. doi:10.1016/j.bcp.2018.12.013
45. Tato-Costa J, Casimiro S, Pacheco T, et al. Therapy-induced cellular senescence induces epithelial-to-mesenchymal transition and increases invasiveness in rectal cancer. *Clin Colorectal Cancer.* 2016;15:170-178.e3. doi:10.1016/j.clcc.2015.09.003
46. Lee SLO, Hong SW, Shin JS, et al. p34SEI-1 inhibits doxorubicin-induced senescence through a pathway mediated by protein kinase C- δ and c-Jun-NH2-kinase 1 activation in human breast cancer MCF7 cells. *Mol Cancer Res.* 2009;7:1845-1853. doi:10.1158/1541-7786.MCR-09-0086
47. Srdic-Rajic T, Santibañez JF, Kanjer K, et al. Iscador Qu inhibits doxorubicin-induced senescence of MCF7 cells. *Sci Rep.* 2017;7:3763. doi:10.1038/s41598-017-03898-0
48. Di X, Shiu RP, Newsham IF, Gewirtz DA. Apoptosis, autophagy, accelerated senescence and reactive oxygen in the response of human breast tumor cells to Adriamycin. *Biochem Pharmacol.* 2009;77:1139-1150. doi:10.1016/j.bcp.2008.12.016
49. Huun J, Lønning PE, Knappskog S. Effects of concomitant inactivation of p53 and pRb on response to doxorubicin treatment in breast cancer cell lines. *Cell Death Discov.* 2017;3:17026. doi:10.1038/cddiscovery.2017.26
50. Jackson JG, Pereira-Smith OM. Primary and compensatory roles for RB family members at cell cycle gene promoters that are deacetylated and downregulated in doxorubicin-induced senescence of breast cancer cells. *Mol Cell Biol.* 2006;26:2501-2510. doi:10.1128/mcb.26.7.2501-2510.2006
51. Elmore LW, Rehder CW, Di X, et al. Adriamycin-induced senescence in breast tumor cells involves functional p53 and telomere dysfunction. *J Biol Chem.* 2002;277:35509-35515. doi:10.1074/jbc.M205477200
52. Bunz F, Dutriaux A, Lengauer C, et al. Requirement for p53 and p21 to sustain G2 arrest after DNA damage. *Science.* 1998;282:1497-1501. doi:10.1126/science.282.5393.1497
53. Fröhlich T, Ndreshkjana B, Muenzner JK, et al. Synthesis of novel hybrids of thymoquinone and artemisinin with high activity and selectivity against colon cancer. *ChemMedChem.* 2017;12:226-234. doi:10.1002/cmdc.201600594
54. Zhou M, Liu X, Li Z, Huang Q, Li F, Li CY. Caspase-3 regulates the migration, invasion and metastasis of colon cancer cells. *Int J Cancer.* 2018;143:921-930. doi:10.1002/ijc.31374
55. El-Mahdy MA, Zhu Q, Wang QE, Wani G, Wani AA. Thymoquinone induces apoptosis through activation of caspase-8 and mitochondrial events in p53-null myeloblastic leukemia HL-60 cells. *Int J Cancer.* 2005;117:409-417. doi:10.1002/ijc.21205
56. Attoub S, Sperandio O, Raza H, et al. Thymoquinone as an anticancer agent: evidence from inhibition of cancer cells viability and invasion in vitro and tumor growth in vivo. *Fundam Clin Pharmacol.* 2013;27:557-569. doi:10.1111/j.1472-8206.2012.01056.x
57. Roepke M, Diestel A, Bajbouj K, et al. Lack of p53 augments thymoquinone-induced apoptosis and caspase activation in human osteosarcoma cells. *Cancer Biol Ther.* 2007;6:160-169.
58. Kundu JKJ, Choi BY, Jeong C-HH, Kundu JKJ, Chun K-SS. Thymoquinone induces apoptosis in human colon cancer HCT116 cells through inactivation of STAT3 by blocking JAK2- and Src-mediated phosphorylation of EGF receptor tyrosine kinase. *Oncol Rep.* 2014;32:821-828. doi:10.3892/or.2014.3223
59. Aslan M, Afşar E, Kırmıloğlu E, Çeker T, Yılmaz Ç. Antiproliferative effects of thymoquinone in MCF-7 breast and HepG2 liver cancer cells: possible role of ceramide and ER stress. *Nutr Cancer.* 2021;73:460-472. doi:10.1080/01635581.2020.1751216

60. Fang Y, Li J, Wu Y, Gui J, Shen Y. Costunolide inhibits the growth of OAW42-a multidrug-resistant human ovarian cancer cells by activating apoptotic and autophagic pathways, production of reactive oxygen species (ROS), cleaved caspase-3 and cleaved caspase-9. *Med Sci Monit.* 2019;25:3231-3237. doi:10.12659/MSM.914029
61. Yan Z, Xu T, An Z, et al. Costunolide induces mitochondria-mediated apoptosis in human gastric adenocarcinoma BGC-823 cells. *BMC Complement Altern Med.* 2019;19:151. doi:10.1186/s12906-019-2569-6
62. Wang C, Youle RJ. The role of mitochondria. *Annu Rev Genet.* 2009;43:95-118. doi:10.1146/annurev-genet-102108-134850
63. Srinivas G, Panicker KR, Pillai MR, Kusumakumary P, Nair MK. Mutant p53 protein, Bcl-2/Bax ratios and apoptosis in paediatric acute lymphoblastic leukaemia. *J Cancer Res Clin Oncol.* 2000;126:62-67. doi:10.1007/s004320050010
64. Argiris A, Cohen E, Karrison T, et al. A phase II trial of perifosine, an oral alkylphospholipid, in recurrent or metastatic head and neck cancer. *Cancer Biol Ther.* 2006;5:766-770. doi:10.4161/cbt.5.7.2874
65. Vaskivuo TE, Stenbäck F, Karhumaa P, Risteli J, Dunkel L, Tapanainen JS. Apoptosis and apoptosis-related proteins in human endometrium. *Mol Cell Endocrinol.* 2000;165:75-83. doi:10.1016/S0303-7207(00)00261-6